Brn3a as a Marker of Retinal Ganglion Cells: Qualitative and Quantitative Time Course Studies in Naïve and Optic Nerve–Injured Retinas

Francisco M. Nadal-Nicolás,[1,2,3] *Manuel Jiménez-López,*[1,3] *Paloma Sobrado-Calvo,*[1] *Leticia Nieto-López,*[1] *Isabel Cánovas-Martínez,*[1] *Manuel Salinas-Navarro,*[1] *Manuel Vidal-Sanz,*[1] *and Marta Agudo*[1,2]

Purpose. To characterize Brn3a expression in adult albino rat retinal ganglion cells (RGCs) in naïve animals and in animals subjected to complete intraorbital optic nerve transection (IONT) or crush (IONC).

Methods. Rats were divided into three groups, naïve, IONT, and IONC. Two-, 5-, 9-, or 14-day postlesion (dpl) retinas were examined for immunoreactivity for Brn3a. Before the injury, the RGCs were labeled with Fluorogold (FG; Fluorochrome, Corp. Denver, CO). Brn3a retinal expression was also determined by Western blot analysis. The proportion of RGCs double labeled with Brn3a and FG was determined in radial sections. The temporal course of reduction in $Brn3a^+$ RGCs and FG^+ RGCs induced by IONC or IONT was assessed by quantifying, in the same wholemounts, the number of surviving FG-labeled RGCs and $Brn3a^+$RGCs at the mentioned time points. The total number of FG^+RGCs was automatically counted in naïve and injured retinas (2 and 5 dpl) or estimated by manual quantification in retinas processed at 9 and 14 dpl. All Brn3a immunopositive RGCs were counted using an automatic routine specifically developed for this purpose. This protocol allowed, as well, the investigation of the spatial distribution of these neurons.

Results. $Brn3a^+$ cells were only present in the ganglion cell layer and showed a spatial distribution comparable to that of FG^+ cells. In the naïve retinal wholemounts the mean (mean ± SEM; $n = 14$) total number of FG^+RGCs and $Brn3a^+$RGCs was 80,251 ± 2,210 and 83,449 ± 4,541, respectively. Whereas in the radial sections, 92.2% of the FG^+RGCs were also $Brn3a^+$, 4.4% of the RGCs were $Brn3a^+FG^-$ and 3.4% were FG^+Brn3a^-. Brn3a expression pattern was maintained in injured RGCs. The temporal course of $Brn3a^+$RGC and FG^+RGC loss induced by IONC or IONT followed a similar trend, but $Brn3a^+$RGCs loss was detected earlier than that of FG^+RGCs. Independent of the marker used to detect the RGCs, it was observed that their loss was quicker and more severe after IONT than after IONC.

Conclusions. Brn3a can be used as a reliable, efficient ex vivo marker to identify and quantify RGCs in control and optic nerve–injured retinas. (*Invest Ophthalmol Vis Sci.* 2009;50:3860–3868) DOI:10.1167/iovs.08-3267

Rodent retinal ganglion cells (RGCs) are widely used to study neurodegenerative processes associated with axonal lesion (Parrilla-Reverter G, et al. IOVS 2004;45:ARVO E-Abstract 911),[1–8] as well as to assay neuroprotective therapies.[9–13] RGCs share their location in the ganglion cell layer with the equally numerous population of displaced amacrine cells,[14–17] making it difficult to distinguish these two types of retinal neurons.[7,13] One of the most common methods of identifying RGCs relies on the use of neuronal tracers applied to their main targets in the brain, the superior colliculi (SCi).[7,11,18–20] Fluorogold (FG; Fluorochrome Corp, Denver, CO) is the tracer of choice for most laboratories,[7,18,21,22] and application of this tracer to both SCi results 1 week later in the labeling of 98.4% and 97.8% of the RGC population in albino and pigmented rats, respectively.[18]

An alternative for identifying RGCs is the immunodetection of proteins specifically expressed by these cells[14,23,24] or in situ hybridization to detect RGC-specific mRNAs. Thy1 is an RGC-specific antigen,[25,26] but it is not a good marker of RGC loss after retinal lesion,[27–29] since its expression pattern may change after retinal injury.[2,27] Immunodetection of Bex1/2 recognizes both RGC bodies and their projections and thus is an appropriate marker for the study of RGC morphologic changes associated to injury.[30] Because of its axonal expression, however, it is not suitable for quantification analysis. In situ hybridization of γ-synuclein is a good approach to identifying RGCs,[31] but this technique impairs double labeling with antibodies, and it is more difficult than immunohistofluorescence protocols. Transgenic approaches have also been used successfully to identify various populations of retinal neurons, including RGCs,[32,33] but this technology is not widely available in rats.

The Brn3 family of POU-domain transcription factors has been shown to play important roles in differentiation, survival, and axonal elongation during the development of murine RGCs.[34] These factors are also emerging as reliable markers for RGCs. For example, Brn3b has been used to identify RGCs in mice[35] and rats,[30] and Brn3a has been shown to be specifically expressed by RGCs that project to the contralateral SCi and dorsal lateral geniculate nucleus in adult mice[36] and has been used to recognize RGCs from rat retinas cultured in vitro.[37] To date, however, there have been no reports analyzing the number of rat RGCs expressing Brn3a, its spatial distribution within

From [1]Departamento de Oftalmología, Facultad de Medicina, Campus Espinardo, Universidad de Murcia, Murcia, Spain; [2]Servicio Murciano de Salud. Hospital Universitario Virgen de la Arrixaca, Fundación para la Formación e Investigación Sanitarias de la Región de Murcia, Murcia, Spain.

[3]Contributed equally to the work and therefore should be considered equivalent authors.

Supported by ISCIII and fondos FEDER: CP003/00119, PI070225, RD07/0062/0001; Fundación Séneca: 04446/GERM/07, 02989/PI/05, and MECSAF-2005-04812.

Submitted for publication December 5, 2008; revised January 7 and 29, 2009; accepted May 20, 2009

Disclosure: **F.M. Nadal-Nicolás**, None; **M. Jiménez-López**, None; **P. Sobrado-Calvo**, None; **L. Nieto-López**, None; **I. Cánovas-Martínez**, None; **M. Salinas-Navarro**, None; **M. Vidal-Sanz**, None; **M. Agudo**, None

The publication costs of this article were defrayed in part by page charge payment. This article must therefore be marked "*advertisement*" in accordance with 18 U.S.C. §1734 solely to indicate this fact.

Corresponding author: Marta Agudo, Servicio Murciano de Salud, FFIS, Departamento de Oftalmología, Facultad de Medicina, Campus Espinardo, Universidad de Murcia, 30100 Murcia, Spain; martabar@um.es.

the retina, or its expression pattern after axonal injury. Thus, in the present studies, using an automatic routine,[18] we quantified the entire population of RGCs expressing Brn3a and examined their spatial distribution within the retina. Moreover, the temporal loss of Brn3a$^+$RGCs induced by IONT or IONC was also examined and compared to the loss of FG-labeled RGCs in the same retinas. Taken together, our results suggest that Brn3a may be used as a reliable marker to identify and quantify RGCs in naïve and axotomized retinas.

Material and Methods

Animal Handling, Groups, and Surgery

Adult female Sprague-Dawley rats (180–220 g body weight) were obtained from the University of Murcia breeding colony. For anesthesia, a mixture of xylazine (10 mg/kg body weight; Rompun; Bayer, Kiel, Germany) and ketamine (60 mg/kg body weight; Ketolar; Pfizer, Alcobendas, Madrid, Spain) was used IP. All experimental procedures were performed in accordance with the ARVO Statement for the Use of Animals in Ophthalmic and Vision Research.

The left optic nerve was intraorbitally injured according to standard procedures in our laboratory (Parrilla-Reverter G, et al. IOVS 2004;45: ARVO E-Abstract 911).[7,8,11,20,38–40] For intraorbital optic nerve transection (IONT), the optic nerve was sectioned 0.5 mm from the optic disc, whereas for intraorbital optic nerve crush (IONC), the optic nerve was crushed for 10 seconds at 3 mm from the optic disc with watchmaker's forceps (Parrilla-Reverter G, et al. IOVS 2004;45:ARVO E-Abstract 911)[8]; the right eyes were used as the control.

RGCs were identified with FG (3% diluted in 10% DMSO-saline) applied to both SCi by using previously described techniques that are standard in our laboratory,[5,11,18,39] 1 week before processing in the naïve group or one week before optic nerve injury in the experimental groups.

Three groups were prepared, one control naïve and two experimental subjected to IONT or IONC; these two were analyzed at 2, 5, 9, or 14 days. The number of retinas analyzed per group, time point, and analysis performed is shown in the results. All animals were labeled with FG, except the four additional naïve animals whose retinas were used to assess whether Brn3a detection was affected by FG-tracing (naïve without FG group, see the Results section) and the animals used for Western blot analysis.

Immunohistofluorescence

All animals were deeply anesthetized and perfused transcardially with 4% paraformaldehyde in 0.1 M phosphate buffer after a saline rinse.

Radial Sections. Immunohistofluorescence analyses were performed as previously described.[38,39] The sections were blocked in 2% donkey serum in phosphate-buffered saline (PBS) with 0.1% Triton-100 (PBST) and incubated overnight a 4°C with goat-anti Brn3a (C-20) antibody (Santa Cruz Biotechnology, Heidelberg, Germany) diluted 1:200 in PBST. Immunoreactivity was detected with Alexa Fluor-568 donkey anti-goat IgG (H$^+$L) antibody (Invitrogen-Molecular Probes, Barcelona, Spain), diluted 1:500 in PBST.

Flatmounted Retinas. Retinas from both eyes were dissected as flattened wholemounts as previously reported.[18] The retinas were permeabilized in PBS 0.5% Triton by freezing them for 15 minutes at −70°C, rinsed in new PBS 0.5% Triton, and incubated overnight at 4°C with goat-antiBrn3a antibody diluted 1:100 in blocking buffer (PBS, 2% bovine serum albumin, 2% Triton). Then, the retinas were washed three times in PBS and incubated for 2 hours at room temperature with the secondary antibody diluted 1:500 in blocking buffer. Finally, they were thoroughly washed in PBS and mounted vitreous side up on subbed slides and covered with antifading solution.

Western Blot Analysis

Western blot analysis was performed as previously described.[38,39] Protein was extracted from freshly dissected retinas of control, IONT, and IONC injured animals (12 and 48 hours [hpl], and 7 dpl, $n = 4$ per group and time point). Brn3a signal was detected with goat-anti Brn3a (C-20) antibody (1:200 in PBS-Tween 0.1%). Secondary detection was performed with horseradish peroxidase donkey anti-goat–conjugated secondary antibody (1:5000, Santa Cruz Biotechnology), visualized by chemiluminescence (Enhanced Chemiluminescence [ECL]; Amersham-GE Health Care Europe GmbH, Barcelona, Spain) and exposure to an x-ray film. As loading control, actin detection was performed with rabbit anti-actin (Sigma-Aldrich, Alcobendas, Madrid, Spain) detected with donkey anti-rabbit-HRP (Santa Cruz Biotechnology).

Retinal Analysis

All wholemounted retinas (left and right eyes) were analyzed for FG and Brn3a signal, acquiring first the FG and then the Brn3a signal. In the naïve group without FG, only Brn3a signal was acquired. To make reconstructions of retinal wholemounts, we photographed the retinas under an epifluorescence microscope (Axioscop 2 Plus; Zeiss Mikroskopie, Jena, Germany) equipped with a computer-driven motorized stage (ProScan H128 Series; Prior Scientific Instruments, Cambridge, UK), controlled by IPP (IPP 5.1 for Windows; Media Cybernetics, Silver Spring, MD), as previously described.[17,18] Reconstructed images were further processed when required (Photoshop CS 8.0.1; Adobe Systems, Inc., San Jose, CA).

Image Processing: Automatic Quantification of the Total Population of FG or Brn3a$^+$RGCs in Wholemounted Retinas

The individual FG-fluorescent images taken for each retinal wholemount were processed after a specific cell-counting subroutine developed by our group,[18,41] and this method was used to automatically quantify FG$^+$RGCs in naïve and injured retinas at 2 and 5 dpl. Briefly, we used the IPP macro language to apply a sequence of filters and transformations to each image to clarify cell limits and to separate individual cells for automatic cell counting previously reported in detail.[18]

Because the Brn3a signal in naïve and injured retinas was clear and strong, an automatic routine was developed to quantify the total number of Brn3a$^+$ nuclei present in flat wholemounted retinas: In a first step, images were converted to 16-bit gray scale to discard the color information. This step was followed by the application of the convolution filter HiGauss (kernel size 7×7) to highlight positive cells. The resultant image data were then filtered with a Sharpen (7×7) filter, which enhances fine detail using the unsharpening masking technique. After that, the image data were filtered again with the LoPass (7×7) filter, which softens the image by blurring the edges and replaces the center pixel with the mean value of its neighborhood. Finally, the resultant images were passed through the HiPass (7×7) filter, which enhances high-frequency information and replaces its center pixel with a value that increases contrast from its neighbors. Cell clusters were separated by two passes of the IPP watershed split morphologic filter, which erodes and dilates objects separating overlapping ones. The nuclei were counted within predetermined parameters to exclude objects that are too large and too small to be RGCs nuclei. Finally, the data of each count were displayed and exported by dynamic data exchange to a spreadsheet (Office Excel 200; Microsoft Corp., Redmond, WA) where the data were filed and saved for further analysis.

Validation of the Brn3a Automatic Counting Method

To validate the Brn3a automatic counting method, three different experienced investigators counted manually, in a masked fashion a total of 26,625 Brn3a$^+$RGCs present in 21 frames, representing different RGC density regions which were randomly selected from six wholemounted naïve retinas. These results were plotted against the counts obtained automatically (26,301 cells), and there was a strong

correlation between both methods (Pearson correlation test, R^2 = 0.98) that validates the automatic quantification of Brn3a$^+$RGCs.

Isodensity Maps

Detailed spatial distribution of FG$^+$RGCs and Brn3a$^+$RGCs over the entire retinas was demonstrated with isodensity maps constructed as previously described.[18,41]

Manual Quantification of FG$^+$RGCs in Wholemounted Retinas

To determine the number of FG$^+$RGCs in injured retinas at 9 or 14 days, we counted the cells manually according to a previously described method,[3,7,11,42] because the presence of microglial cells transcellularly labeled with FG interfered with the automatic counting.[43] The fusiform body and the dot-like FG accumulations in microglial cells make it possible to tell them apart from the typical appearance of FG-labeled RGCs.[5] FG$^+$RGCs were counted by three investigators blinded to procedure in photographs of 12 rectangular areas (each 0.1515 mm^2) of each retina, three in each quadrant. The first image was taken at 0.875 mm from the optic disc and the remaining two 1 mm apart from each other. The number of labeled cells in the 12 photographs was averaged and the mean number of FG$^+$RGCs per area unit was extrapolated to the total area of each retina, to estimate the total number of FG$^+$RGCs present in each one.

Retinal Area Measurement

The area of each wholemounted retina was measured on the high-resolution photomontage image of the whole retina with the computer program (IPP; Media Cybernetics) calibrated off the stage movement.

Assessment of the Brn3a Expression Pattern in Naïve and Injured Retinas and of the Percentage of Cells Positive for FG, Brn3a, or Both Markers in Naïve Retinas

Images from radial sections of naïve and IONT- and IONC-injured retinas processed at 2, 5, 9, or 14 dpl were taken randomly from different areas of the retina, acquiring FG and Brn3a signal for each one. Five retinas from experimental animals were analyzed per time point and lesion and six from control ones. Images from each signal were coupled (Photoshop CS 8.0.1; Adobe Systems, Inc., San Jose, CA) to assess for colocalization. The number of cells positive only for FG (blue signal), only for Brn3a (red signal), or for both markers (colocalization), was counted in naïve retinas. In each image, there were 26 ± 11 (mean ± SEM) RGCs, thus at least 10 images per retina were analyzed (2192 RGCs were counted in total). The percentage of positive cells for either marker combination was calculated in relation to the total number of cells counted, which was considered 100%.

Statistical Analyses

To compare values from both retinas of different rats and the number of FG or Brn3a positive RGCs, we used the Mann-Whitney test (Statistix ver.10; Analytical Software, Tallahassee, FL). Cell counts obtained by the automated method were compared with those obtained with the manual method using the Pearson correlation test (SigmaStat for Windows, ver. 3.11; Systat Software, Inc., Richmond, CA). Differences were considered significant at $P < 0.05$.

Results

Expression Pattern of Brn3a$^+$ Cells in Naïve Retinas: Quantification of the Whole Population of Brn3a$^+$RGCs and of FG$^+$RGCs

Fluorescence microscopy of wholemounted naïve retinas immunodetected for Brn3a showed many stained nuclei in the ganglion cell layer distributed throughout the retina (Fig. 1A). An automatic routine, which allows rapid and reliable counting, was used to quantify the whole population of Brn3a$^+$RGCs. Moreover, once all the RGCs are counted, it is possible to analyze their spatial distribution in the retina by means of detailed isodensity maps[18,41] (Fig. 1B). These same retinas had been previously traced with FG (Fig. 1C). Thus, for comparison, the number of FG$^+$RGCs was also counted (Table 1). In these retinas, the averaged total number of Brn3a$^+$RGCs (84,682 ± 7,601; mean ± SEM; n = 14) was not significantly different from the mean total number of FG$^+$RGCs (80,252 ± 2,210; Table 1). To document that retrograde tracing with FG did not interfere with Brn3a immunodetection, in eight naïve retinas without FG, Brn3a$^+$RGCs were counted as well. In these retinas, the mean total number of Brn3a$^+$RGCs (84,813 ± 5,668) was comparable to that of the cells counted in the group of naïve retinas prelabeled with FG, as described earlier, thus indicating that previous tracing with FG does not impair the detection of Brn3a or the quantification routine.

Detailed isodensity maps were constructed to examine the spatial distribution of FG$^+$RGCs and Brn3a$^+$RGCs in the retina. These maps showed that these two populations always adopted a comparable spatial distribution within the same retinas (Figs. 1C, 1D), with high RGC densities in the dorsal area resembling a visual streak, which is a typical feature of RGC spatial distribution in the rat retina.[18]

To further demonstrate that Brn3a was expressed by RGCs, we analyzed radial sections of FG-traced retinas immunostained for Brn3a. The nuclear signal of Brn3a was circumscribed to the ganglion cell layer, and most of the Brn3a$^+$ cells

Table 1. Population of Brn3a$^+$ and FG$^+$RGCs in Naïve and Optic Nerve Injured Retinas

Naïve (n = 14)					
Brn3a$^+$RGCs	83,449 ± 4,541				
FG$^+$RGCs	80,251 ± 2,210				
IONT	**RE (n = 32)**	**48 hpl (n = 8)**	**5 dpl (n = 8)**	**9 dpl (n = 8)**	**14 dpl (n = 8)**
Brn3a$^+$RGCs	82,434 ± 4,802	65,120 ± 6,439*†	29,463 ± 5,552*†	17,335 ± 7,068*	4,778 ± 1,332*†
FG$^+$RGCs	82,078 ± 3,283	80,899 ± 4,406	68,943 ± 8,370*	25,299 ± 3,989*	10,598 ± 2,785*
IONC	**RE (n = 32)**	**48 hpl (n = 8)**	**5 dpl (n = 8)**	**9 dpl (n = 8)**	**14 dpl (n = 8)**
Brn3a$^+$RGCs	85,047 ± 3,696	79,013 ± 8,435	40,690 ± 6,227*†	21,869 ± 7,578*	10,176 ± 2,940*†
FG$^+$RGCs	82,535 ± 2,672	80,101 ± 3,477	73,553 ± 3,039	36,974 ± 7,209*	21,117 ± 5,824*

Number (mean ± SEM) of RGCs immunodetected for Brn3a or labeled with FG per retina. The number of FG$^+$RGCs present in naïve, control right eyes, at 2 days and 5 days post-IONT or IONC retinas was counted automatically from retinal wholemounts. In retinas processed at 9 and 14 days post-IONT or IONC, the number of FG$^+$RGCs was counted manually, and the total population of these cells estimated. The number of Brn3a$^+$RGCs in the same retinas was counted automatically in all groups. Note that the mean number of cells FG$^+$ or Brn3a$^+$ present in the right-eye untouched retinas of each injury group did not differ from the number of RGCs counted in naïve retinas.

* Statistically significant when compared to naïve and control fellow right eye.

† Statistically significant when compared to the number of FG$^+$RGCs at the same time point. Mann-Whitney test $P < 0.05$.

were also FG^+ (Fig. 2A). Quantification of the number of cells positive for either marker showed that in naïve retinas 92.2% of FG^+RGCs also expressed Brn3a, 4.4% of the retinal cells expressing Brn3a were not labeled with FG, and 3.4% of FG^+RGCs did not express Brn3a (Fig. 3A). Taken together, these results indicate that Brn3a is expressed in most of the FG^+RGCs and suggest that Brn3a may be used as a marker to identify RGCs in naïve retinas.

Brn3a Expression Pattern in Optic Nerve–Injured Adult Rat Retinas: Qualitative Analysis in Radial Sections

We next performed a group of experiments designed to determine (1) whether Brn3a expression in RGCs was maintained after optic nerve injury and (2) whether other retinal cells would start to express Brn3a as a result of the lesion. Radial cryostat sections of FG-traced retinas undergoing IONT or IONC examined at different times postlesion showed the typical progression of RGC loss induced by optic nerve in-

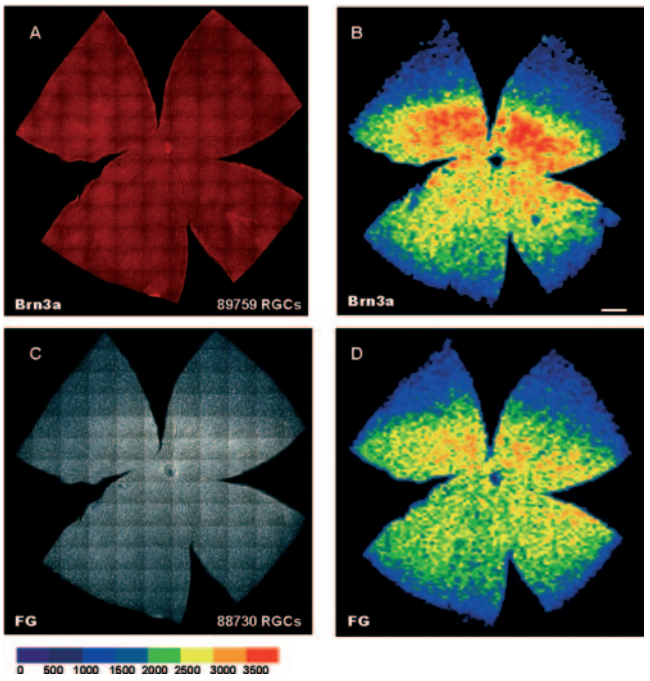

FIGURE 1. Distribution of Brn3a immunopositive RGCs and FG-labeled RGCs in the naïve adult rat retina. Wholemount of a representative SD naïve rat retina showing Brn3a-immunopositive (**A**) and FG-labeled (**C**) RGCs. For these images, isodensity maps were generated (**B**, **D**, respectively). The maps are filled contour plots generated by assigning a color code to each one of the 64 subdivisions of each individual frame according to its RGC density within a 28-step color-scale range from 0 (*purple*) to 3500 or higher (*red*) RGCs/mm^2. The spatial distribution of $Brn3a^+$ (**A**, **B**) and FG^+ (**C**, **D**) RGCs was similar, and in both cases the isodensity maps detected the high RGC– density area along the dorsal retina resembling a visual streak. The number of RGCs detected with Brn3a or FG or is shown in (**A**) and (**C**), respectively. The dorsal pole is situated at the 12-o'clock orientation. Bar, 1 mm.

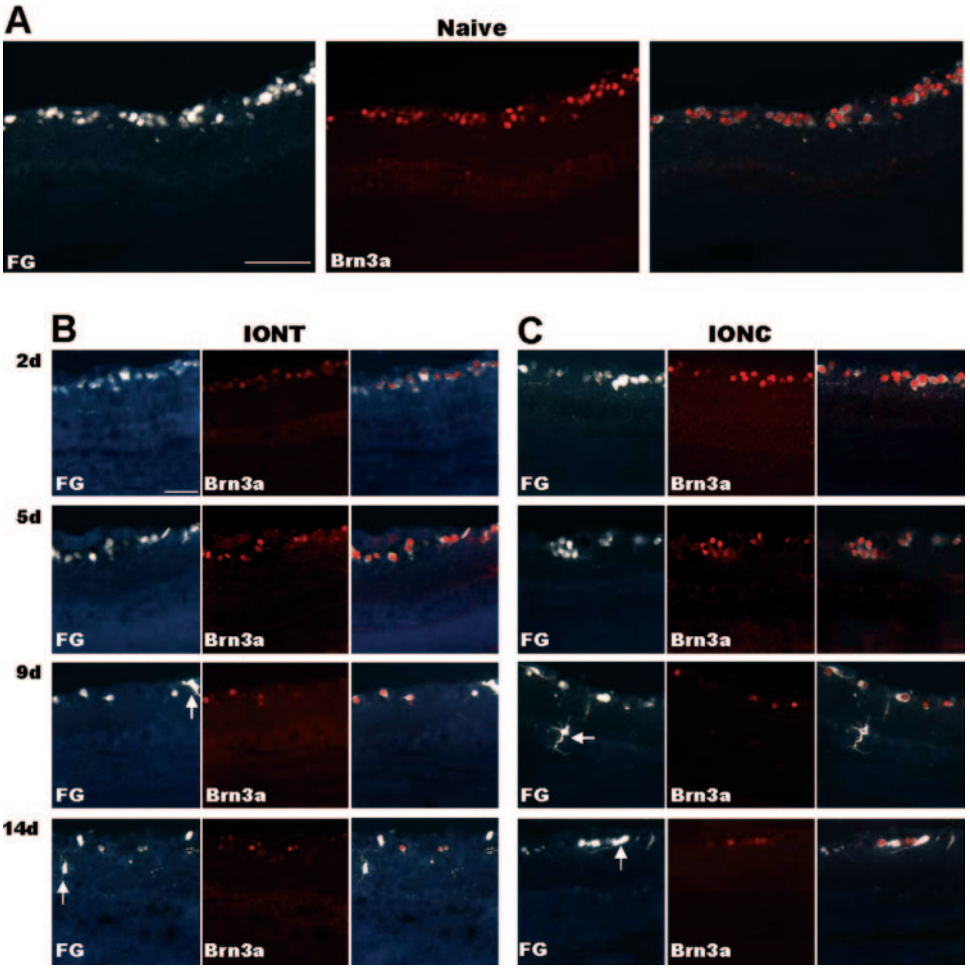

FIGURE 2. Brn3a expression pattern in naïve and injured retinas: qualitative analysis on radial sections. (**A–C**) Radial sections of FG-labeled retinas immunodetected for Brn3a. (**A**) Naïve retinas, (**B**) IONT-injured retinas at increasing postlesion times, and (**C**) IONC-injured retinas at the same postlesion times. *Left*: FG signal (*blue*); *middle*: Brn3a signal (*red*); *right*: superimposition of both images. The Brn3a expression is restricted to the ganglion cell layer and predominantly colocalizes with FG-labeled RGCs. Although at 9 and 14 days after IONT or IONC some FG-labeled microglial cells are present (*arrows*), Brn3a signal was never observed in these cells. Bar: 100 μm.

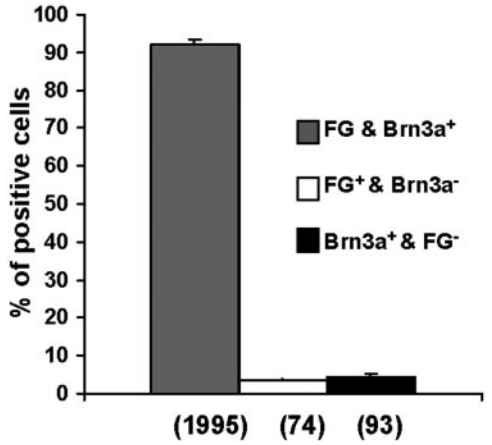

FIGURE 3. Percentage of RGCs positive for FG and Brn3a in naïve retinas. The percentage of RGCs labeled with FG that expressed Brn3a, RGCs labeled with FG that did not express Brn3a, and RGCs that express Brn3a but were not labeled with FG. The number of counted cells is shown in parentheses (n = 6 retinas). The percentage of positive cells for either marker combination was calculated in relation to the total number of cells counted.

jury.[7,8,11] These same sections also showed that after IONT or IONC, Brn3a was expressed in the ganglion cell layer (Figs. 2B, 2C) and, as for the naïve retinas, its signal frequently colocalized with FG. This expression pattern was maintained as the postlesion time increased in all analyzed retinas, and it is worth noting that Brn3a expression was not shut down immediately after either axotomy. Taken together this analysis documented that Brn3a was expressed by most of the FG-labeled RGCs, and also that its expression was always circumscribed to RGCs, not only in naïve retinas, as described earlier, but also after optic nerve injury. Therefore, Brn3a may be used as a reliable and efficient marker to detect RGCs after IONT and IONC.

Brn3a Expression Pattern in Optic Nerve–Injured Adult Rat Retinas: Quantitative Analysis in Wholemounts

Once it was established that Brn3a was expressed in axotomized RGCs and that axotomy had not triggered the upregulation of Brn3a in other retinal neurons, we quantified the temporal loss of Brn3a$^+$RGCs in wholemounts of retinas after IONT or IONC, using the newly developed automatic routine. This analysis was performed in retinas that had been previously labeled with FG, and thus it was possible to compare the time course of RGC loss with both markers (Fig. 4). In the retinas examined at 9 or 14 dpl, in addition to FG-labeled RGCs, there were also FG-labeled microglial cells; however, these were not seen under the rhodamine filter in the corresponding images that allowed observation of Brn3a$^+$RGCs (Figs. 4B, 4C).

The mean total number of FG$^+$RGCs and Brn3a$^+$RGCs present in the same retinas after IONT or IONC decreased with increasing survival intervals (Table 1, Fig. 5). After IONT the loss of Brn3a$^+$RGCs became statistically significant at 2 dpl (Mann-Whitney test, $P < 0.05$), when 65,120 ± 6,439 cells (mean ± SEM; n = 8) were counted. At this time point, there was a significant difference between the number of Brn3a$^+$RGCs and the number of FG$^+$RGCs (80,899 ± 4,406; n = 8), as the latter do not differ from the total number of FG$^+$RGCs in naïve retinas. This finding is in agreement with previous studies indicating that the loss of FG-labeled RGCs was not significant until 5 dpl.[1,11,44] The loss of RGCs labeled with both markers progressed with time after IONT, although it always appeared more severe when Brn3a expression was analyzed (Table 1, Figs. 4, 5). After IONC, the loss of Brn3a$^+$RGCs first became statistically significant at 5 dpl, when 40,690 ± 6,227 Brn3a$^+$RGCs were counted (mean ± SEM; n = 8), whereas the mean total number of FG$^+$RGCs was 73,553 ± 3,039 (mean ± SEM; n = 8). The latter did not differ from the naïve or right fellow retinas, as previously reported (Parrilla-Reverter G, et al. IOVS 2004;45:ARVO E-Abstract 911).[8] As it was observed after IONT, the loss of Brn3a expression induced by IONC appeared earlier than the clearance of FG-labeled RGCs (Table 1, Figs. 4, 5). The loss of RGCs analyzed by FG-labeling or Brn3a expression after IONC appeared slower than after IONT (Table 1, Figs. 4, 5).

The quantitative analysis was paralleled with inspection of the isodensity maps that showed the spatial retinal distribution of Brn3a$^+$RGCs. In the group of IONT retinas, as the survival intervals progressed, there was a tendency for warm colors to disappear throughout the whole retinal surface reflecting the diffuse loss of Brn3a$^+$RGCs. A similar time trend was observed for the IONC injured retinas, but this was less severe (Figs. 4D, 4E). For instance, by 2 dpl, the loss of Brn3a$^+$RGCs was already apparent around the dorsal retina, where Brn3a$^+$RGCs adopt a typical high-density area (Fig. 4D), and by 5 dpl the loss of Brn3a$^+$RGCs appeared diffuse and was spread throughout the retina (Fig. 4E).

Brn3a Regulation after Optic Nerve Transection and Optic Nerve Crush

After determining that Brn3a was expressed by most FG$^+$RGCs in naïve and optic nerve–injured retinas we assessed, by means of Western blot analysis, the regulation of Brn3a protein in whole retinal extracts. The expression of this transcription factor decreased over time, both after IONT and IONC (Fig. 6), in agreement with our previous report,[38] where it was shown that the mRNA of Brn3a is downregulated by axotomy.

DISCUSSION

In the present studies, we have demonstrated that Brn3a is expressed by most of the FG$^+$RGCs, both in naïve and optic nerve–injured retinas. Importantly, we have also shown that Brn3a expression pattern does not change after retinal injury. Brn3a was detected in Western blot assays from protein extracts of the entire retina. This result is important because RGCs represent less than 1% of the retinal cell population, and RGC-specific proteins are highly diluted in whole retinal extracts. This dilution may explain why, even though in naïve retinas almost all FG-labeled RGCs were Brn3a$^+$, the signal was weak (compare Brn3a with actin bands in Fig. 6). Our results also demonstrate that the levels of Brn3a protein decreased with time after IONT or IONC, in agreement with the quantitative data shown in this study and with our previous array analyses.[38] Brn3a expression was almost undetectable at 7 dpl; however, even at longer survival times, the Brn3a$^+$RGCs were detectable in the retina (Fig. 4, 5). This apparent discrepancy may be explained by the dilution effect, which increased with longer survival intervals, as fewer RGCs remained. Finally, it is possible that the detection of Brn3a using this approach may allow in future experiments the correlation of injury-induced RGC loss and the protection afforded by neuroprotective treatments.

In our study, Brn3a immunodetection in retinal wholemounts permitted the quantification of the total number of Brn3a$^+$RGCs using an automatic routine specifically developed for this purpose. This approach is facilitated by the fact that the Brn3a signal is nuclear.[36,45] This is an advantage over Bex1/2[30] and neurofilament antibodies,[46] which are expressed in the

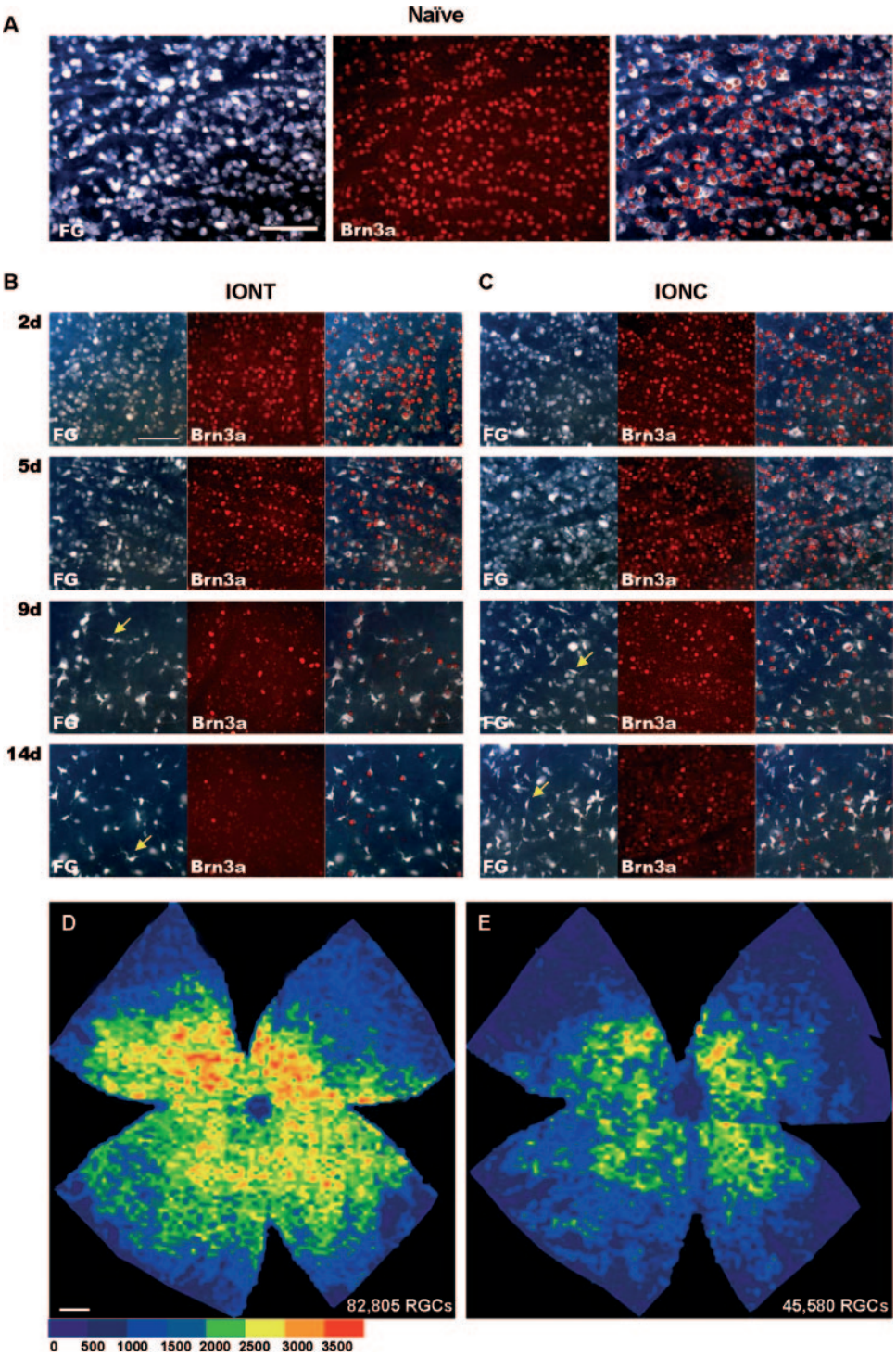

FIGURE 4. Detection of FG and Brn3a positive RGCs in flatmounted naïve and optic nerve–injured retinas. (**A–C**) Fluorescent micrographs from flatmounted retinas labeled with FG and immunoreacted for Brn3a. (**A**) Naïve retinas; (**B**) IONT-injured retinas at increasing postlesion survival intervals; (**C**) IONC-injured retinas at the same postlesion times. *Left*: FG signal (*blue*); *middle*: Brn3a signal (*red*); *right*: superimposition of both images. Brn3a signal predominantly colocalizes with FG-labeled RGCs. *Arrows*: microglial cells transcellularly labeled with Fluorogold. (**D**, **E**) Isodensity maps of wholemounted retinas immunodetected for Brn3a 2 and 5 days after IONC, respectively. The number of Brn3a$^+$RGCs in each retina is shown in the images. RGC density ranged from 0 (*purple*) to 3500 or higher (*red*) RGCs/mm^2. The dorsal pole is situated at the 12-o'clock orientation. Bar: (**A–C**) 200 μm, (**D**) 1 mm.

cell bodies and axons of RGCs and thus cannot be used for RGC quantification analysis.

The mean total number of Brn3a$^+$RGCs counted in the naïve retinas in our experiments are comparable to other studies investigating the number of RGCs in albino rats using different approaches, including counting optic nerve axons,[47] stereological procedures,[48] or sampling the retina and estimating the number of FG-traced RGCs.[21,49,50] Moreover, we show that in the same naïve retinas the numbers of Brn3a$^+$RGCs (83,449.3 ± 4,541) and FG$^+$RGCs (80,251 ± 2,210) are similar. This is consistent with a recent report[18] showing that the population of FG$^+$RGCs in SD rats was 81,486 ± 4,340 (n = 37; Table 3 in Ref. 17). Furthermore, the retinal spatial distribution of Brn3a$^+$RGCs coincides with the typical distribution of FG$^+$RGCs as shown here and previously reported.[18]

At present, we have no clear explanation for the 4.4% of the Brn3a$^+$FG$^-$ cells or for the 3.4% of FG$^+$Brn3a$^-$ RGCs that were observed in radial sections of the naïve retinas. It is possible that a small proportion of the Brn3a$^+$ nuclei are those of displaced amacrine cells that would not be directly affected by optic nerve injury. Indeed, in our naïve wholemount counts, there were on average approximately 2000 to 3000 Brn3a$^+$FG$^-$ cells. Alternatively, this could represent a small proportion of RGCs that did not get retrogradely labeled with

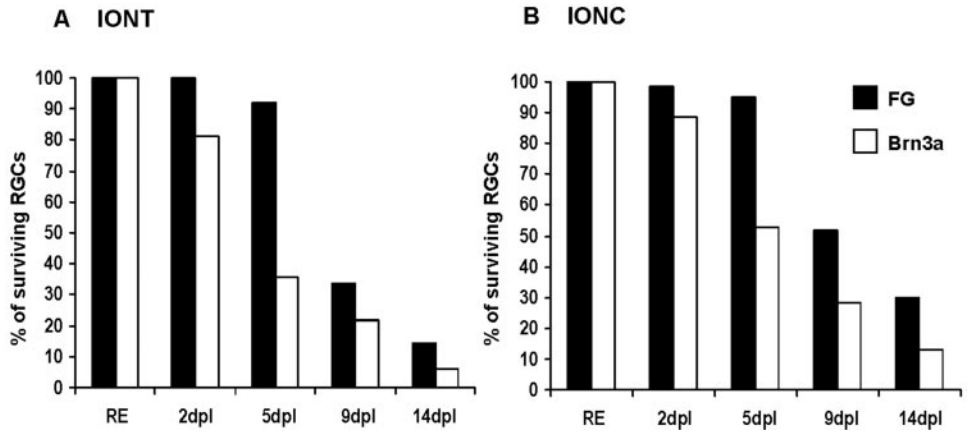

FIGURE 5. Temporal loss of FG^+RGCs and $Brn3a^+$RGCs after intraorbital optic nerve transection (IONT) or intraorbital optic nerve crush (IONC). Percentage of surviving RGCs labeled with FG or immunodetected for Brn3a after IONT (**A**) or IONC (**B**). The percentage of surviving RGCs in experimental retinas (left eye) was referred to their right control retinas, which were arbitrarily considered 100%. The number of retinas analyzed was eight for each group and time point.

FG from both SCi. The small population (3.4%) of FG^+Brn3a^- RGCs could account for the RGCs that projected ipsilaterally as well as for those that project contralaterally to subcortical centers not involved in mediating cortical vision, all of which, in mice, have been reported to be $Brn3a^-$.[36] Of interest, although the number of $Brn3a^+$RGCs in the retina illustrated in Figure 1A was only 1029 cells greater than the number of FG^+RGCs, the isodensity map revealed that these cells were concentrated in the typical region of high RGC density on the dorsal retina (Fig. 1B). This result could be due to the high density of the cells, which indicates that in this area there may be more than one stratum of RGCs (Fig. 4A). Because the Brn3a signal was nuclear, the distances between the positive nuclei were wider, allowing easier discrimination.

We have also analyzed the temporal RGC loss after intraorbital optic nerve transection or crush using both markers. Our data on FG^+RGC loss agrees with previous reports by several groups[1,44] including our laboratory (Parrilla-Reverter G, et al. IOVS 2004;45:ARVO E-Abstract 911),[8,11] showing that increasing survival intervals results in progressive loss of FG-labeled RGCs. Moreover, our data (Fig. 5) are also consistent with previous reports in that IONT[11] induces an earlier, quicker, and more severe loss than IONC does (Parrilla-Reverter G, et al. IOVS 2004;45:ARVO E-Abstract 911).[8] We have also shown for the first time the temporal loss of Brn3a expression in the same retinas, an analysis that was made possible by using an automatic routine to count all $Brn3a^+$RGCs rather than sampling and estimating. This is an advantage over FG-labeled injured retinal analyses because, in these, the presence of transcellularly labeled microglial cells impairs the automatic quantification. Moreover, detailed isodensity maps of $Brn3a^+$RGCs allowed us to observe for the first time how the progression of axotomy-induced RGC loss affected typical RGC spatial distribution within the retina (Figs. 4D, 4E). The loss of RGCs appeared diffuse, affecting first the area where RGCs were more densely concentrated over the superior retina, and then diffusely affecting the rest of the entire retina, so that by 2 weeks after injury, there was a clear loss of RGCs over the entire retina. As mentioned earlier, this loss of $Brn3a^+$RGCs occurred earlier and was faster and more severe in the group of retinas that underwent IONT when compared with those that underwent IONC.

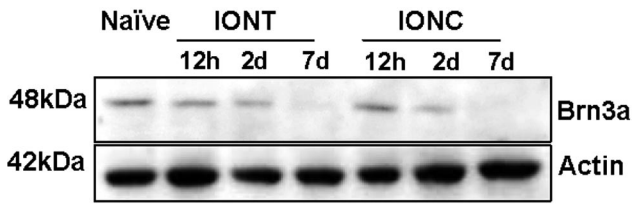

FIGURE 6. Brn3a expression was downregulated in the retina after optic nerve transection and optic nerve crush. Western blot analysis shows that Brn3a protein expression decreased over time in retinas undergoing either IONT or IONC, compared with naïve retinas. Actin signal was used as the loading control.

The temporal loss of Brn3a expression was observed much earlier than the loss of FG labeling. This difference has been also described when Thy1 has been used as an RGC marker in injured retinas.[2,28,29] However, the main concern of Thy1 as a marker of injured RGCs is not that its expression decreases before the loss of FG^+RGCs, but (1) that this decrease does not correlate with RGC death, as Thy1 expression shuts down in mice $Bax^{-/-}$, in which RGCs are resistant to IONC[29] and (2) that on retinal injury, it is expressed by Müller cells.[27] Thy1 is a surface protein, whereas Brn3a is a transcription factor, it is reasonable to think that their molecular functions are quite different. In fact, little is known about the role of Thy1 in RGCs, and to our knowledge there are no reports linking Thy1 to survival. Of importance, it has been described that Brn3a has a survival function antagonizing p53 activation of two proapoptotic proteins, Noxa and Bax,[51,52] and through the activation of survival genes, such as *Bcl-2*[53] or *Hsp27*.[54]

Therefore, it is tempting to suggest that the loss of Brn3a expression happens earlier because it reflects a commitment to death triggered by optic nerve injury and thus precedes the disappearance of the FG-labeled RGCs by phagocytic clearance. This notion agrees with the fact that several proapoptotic proteins, expressed by optic nerve–injured RGCs are upregulated as soon as 12 hpl, peaking at 48 hpl.[38,39] In this sense, as Brn3a is an endogenous marker of RGCs, its expression level may reflect the physiological state of an RGC, diminishing as the cell enters apoptosis. This possibility is further supported by the different temporal course of $Brn3a^+$RGC loss after IONT or IONC, which, as it happens when quantifying the loss of FG^+RGCs, is slower after IONC. This result points out that the loss of Brn3a expression is linked to the well-being of RGCs, since these survive longer after ON crush than after ON transection.[8,11] In contrast, the disappearance of FG-labeled RGCs occurs when activated microglial cells phagocytose the RGC debris, thus delaying the clearing of FG from the tissue.

In summary, we have characterized the expression pattern of Brn3a in adult albino rat retinas, both naïve and injured, and found that Brn3a was a good marker for reliably identifying RGCs. An automatic routine allowed the quantification of the whole population of $Brn3a^+$RGCs present in naïve and optic nerve–injured retinas. Our results indicate that the loss of RGCs induced by IONT or IONC is identified earlier when these cells

are detected by Brn3a expression rather than by FG-labeling, indicating that the downregulation of Brn3a expression precedes the disappearance of FG-traced RGCs from the tissue that follows IONT and IONC. Finally, Brn3a may be useful for other experiments including the use of its promoter for the specific delivery of genes to RGCs, or the correlation of RGC loss in Western blot assays.

References

1. Berkelaar M, Clarke DB, Wang YC, Bray GM, Aguayo AJ. Axotomy results in delayed death and apoptosis of retinal ganglion cells in adult rats. *J Neurosci.* 1994;14:4368–4374.
2. Chidlow G, Casson R, Sobrado-Calvo P, Vidal-Sanz M, Osborne NN. Measurement of retinal injury in the rat after optic nerve transection: an RT-PCR study. *Mol Vis.* 2005;11:387–396.
3. Lafuente MP, Villegas-Perez MP, Selles-Navarro I, Mayor-Torroglosa S, Miralles dI, Vidal-Sanz M. Retinal ganglion cell death after acute retinal ischemia is an ongoing process whose severity and duration depends on the duration of the insult. *Neuroscience*. 2002;109: 157–168.
4. Vidal-Sanz M, Lafuente M, Sobrado-Calvo P, et al. Death and neuroprotection of retinal ganglion cells after different types of injury. *Neurotox Res.* 2000;2:215–227.
5. Vidal-Sanz M, Lafuente MP, Mayor S, de Imperial JM, Villegas-Perez MP. Retinal ganglion cell death induced by retinal ischemia: neuroprotective effects of two alpha-2 agonists. *Surv Ophthalmo*l. 2001;45(suppl 3)S261–S267.
6. Villegas-Perez MP, Vidal-Sanz M, Lund RD. Mechanism of retinal ganglion cell loss in inherited retinal dystrophy. *Neuroreport.* 1996;7:1995–1999.
7. Villegas-Perez MP, Vidal-Sanz M, Rasminsky M, Bray GM, Aguayo AJ. Rapid and protracted phases of retinal ganglion cell loss follow axotomy in the optic nerve of adult rats. *J Neurobiol.* 1993;24:23–36.
8. Parrilla-Reverter G, Agudo M, Sobrado-Calvo P, et al. Neuroprotective effect of Neurotrophin4, Brain derived neurotrophic factor and ciliary neurotrophic factor against intraorbital nerve crush induced retinal ganglion cell loss: a quantitative in vivo study. *Exp Eye Res.* 2009. doi: 10.1016/j.exer.2009.02.015.
9. Bray GM, Villegas-Perez MP, Vidal-Sanz M, Aguayo AJ. The use of peripheral nerve grafts to enhance neuronal survival, promote growth and permit terminal reconnections in the central nervous system of adult rats. *J Exp Biol.* 1987;132:5–19.
10. Lafuente MP, Villegas-Perez MP, Sobrado-Calvo P, Garcia-Aviles A, Miralles dI, Vidal-Sanz M. Neuroprotective effects of alpha(2)-selective adrenergic agonists against ischemia-induced retinal ganglion cell death. *Invest Ophthalmol Vis Sci*. 2001;42:2074–2084.
11. Peinado-Ramon P, Salvador M, Villegas-Perez MP, Vidal-Sanz M. Effects of axotomy and intraocular administration of NT-4, NT-3, and brain-derived neurotrophic factor on the survival of adult rat retinal ganglion cells. a quantitative in vivo study. *Invest Ophthalmol Vis Sci.* 1996;37:489–500.
12. Vidal-Sanz M, De la Villa P, Aviles-Trigueros M, et al. Neuroprotection of retinal ganglion cell function and their central nervous system targets. *Eye.* 2007;21:S42–S45.
13. Villegas-Perez MP, Vidal-Sanz M, Bray GM, Aguayo AJ. Influences of peripheral nerve grafts on the survival and regrowth of axotomized retinal ganglion cells in adult rats. *J Neurosci.* 1988;8:265–280.
14. Drager UC, Olsen JF. Ganglion cell distribution in the retina of the mouse. *Invest Ophthalmol Vis Sci.* 1981;20:285–293.
15. Jeon CJ, Strettoi E, Masland RH. The major cell populations of the mouse retina. *J Neurosci.* 1998;18:8936–8946.
16. Perry VH. Evidence for an amacrine cell system in the ganglion cell layer of the rat retina. *Neuroscience.* 1981;6:931–944.
17. Perry VH, Henderson Z, Linden R. Postnatal changes in retinal ganglion cell and optic axon populations in the pigmented rat. *J Comp Neurol.* 1983;219:356–368.
18. Salinas-Navarro M, Mayor-Torroglosa S, Jimenez-Lopez M, et al. A computerized analysis of the entire retinal ganglion cell population and its spatial distribution in adult rats. *Vision Res.* 2009;49:115–126.
19. Thanos S, Vidal-Sanz M, Aguayo AJ. The use of rhodamine-B-isothiocyanate (RITC) as an anterograde and retrograde tracer in the adult rat visual system. *Brain Res.* 1987;406:317–321.
20. Vidal-Sanz M, Villegas-Perez MP, Bray GM, Aguayo AJ. Persistent retrograde labeling of adult rat retinal ganglion cells with the carbocyanine dye diI. *Exp Neurol.* 1988;102:92–101.
21. Danias J, Shen F, Kavalarakis M, et al. Characterization of retinal damage in the episcleral vein cauterization rat glaucoma model. *Exp Eye Res.* 2006;82:219–228.
22. Wang S, Villegas-Perez MP, Vidal-Sanz M, Lund RD. Progressive optic axon dystrophy and vascular changes in rd mice. *Invest Ophthalmol Vis Sci.* 2000;41:537–545.
23. Canola K, Angenieux B, Tekaya M, et al. Retinal stem cells transplanted into models of late stages of retinitis pigmentosa preferentially adopt a glial or a retinal ganglion cell fate. *Invest Ophthalmol Vis Sci.* 2007;48:446–454.
24. McKerracher L, Vallee RB, Aguayo AJ. Microtubule-associated protein 1A (MAP 1A) is a ganglion cell marker in adult rat retina. *Vis Neurosci.* 1989;2:349–356.
25. Barnstable CJ, Drager UC. Thy-1 antigen: a ganglion cell specific marker in rodent retina. *Neuroscience.* 1984;11:847–855.
26. Perry VH, Morris RJ, Raisman G. Is Thy-1 expressed only by ganglion cells and their axons in the retina and optic nerve? *J Neurocytol.* 1984;13:809–824.
27. Dabin I, Barnstable CJ. Rat retinal Muller cells express Thy-1 following neuronal cell death. *Glia.* 1995;14:23–32.
28. Huang W, Fileta J, Guo Y, Grosskreutz CL. Downregulation of Thy1 in retinal ganglion cells in experimental glaucoma. *Curr Eye Res.* 2006;31:265–271.
29. Schlamp CL, Johnson EC, Li Y, Morrison JC, Nickells RW. Changes in Thy1 gene expression associated with damaged retinal ganglion cells. *Mol Vis.* 2001;7:192–201.
30. Bernstein SL, Koo JH, Slater BJ, Guo Y, Margolis FL. Analysis of optic nerve stroke by retinal Bex expression. *Mol Vis.* 2006;12: 147–155.
31. Surgucheva I, Weisman AD, Goldberg JL, Shnyra A, Surguchov A. Gamma-synuclein as a marker of retinal ganglion cells. *Mol Vis.* 2008;14:1540–1548.
32. Feng G, Mellor RH, Bernstein M, et al. Imaging neuronal subsets in transgenic mice expressing multiple spectral variants of GFP. *Neuron.* 2000;28:41–51.
33. Raymond ID, Vila A, Huynh UC, Brecha NC. Cyan fluorescent protein expression in ganglion and amacrine cells in a thy1-CFP transgenic mouse retina. *Mol Vis.* 2008;14:1559–1574.
34. Wang SW, Mu X, Bowers WJ, et al. Brn3b/Brn3c double knockout mice reveal an unsuspected role for Brn3c in retinal ganglion cell axon outgrowth. *Development.* 2002;129:467–477.
35. Buckingham BP, Inman DM, Lambert W, et al. Progressive ganglion cell degeneration precedes neuronal loss in a mouse model of glaucoma. *J Neurosci.* 2008;28:2735–2744.
36. Quina LA, Pak W, Lanier J, et al. Brn3a-expressing retinal ganglion cells project specifically to thalamocortical and collicular visual pathways. *J Neurosci.* 2005;25:11595–11604.
37. Johnson TV, Martin KR. Development and characterization of an adult retinal explant organotypic tissue culture system as an in vitro intraocular stem cell transplantation model. *Invest Ophthalmol Vis Sci.* 2008;49:3503–3512.
38. Agudo M, Pérez-Marín M, Lönngren U, et al. Time course profiling of the retinal transcriptome after optic nerve transection and optic nerve crush. *Mol Vis.* 2008;14:1050–1063.
39. Agudo M, Perez-Marin MC, Sobrado-Calvo P, et al. Immediate upregulation of proteins belonging to different branches of the apoptotic cascade in the retina after optic nerve transection and optic nerve crush. *Invest Ophthalmol Vis Sci.* 2009;50:424–431.
40. Vidal-Sanz M, Bray GM, Villegas-Perez MP, Thanos S, Aguayo AJ. Axonal regeneration and synapse formation in the superior colliculus by retinal ganglion cells in the adult rat. *J Neurosci.* 1987; 7:2894–2909.
41. Salinas-Navarro M, Jimenez-Lopez M, Valiente-Soriano F, et al. Retinal ganglion cell population in adult albino and pigmented mice: a computerised analysis of the entire population and its spatial distribution. *Vision Res.* 2009;49:637–649.

42. Lafuente MP, Villegas-Perez MP, Mayor S, Aguilera ME, Miralles dI, Vidal-Sanz M. Neuroprotective effects of brimonidine against transient ischemia-induced retinal ganglion cell death: a dose response in vivo study. *Exp Eye Res.* 2002;74:181–189.
43. Kobbert C, Apps R, Bechmann I, Lanciego JL, Mey J, Thanos S. Current concepts in neuroanatomical tracing. *Prog Neurobiol.* 2000;62:327–351.
44. Mansour-Robaey S, Clarke DB, Wang YC, Bray GM, Aguayo AJ. Effects of ocular injury and administration of brain-derived neurotrophic factor on survival and regrowth of axotomized retinal ganglion cells. *Proc Natl Acad Sci USA.* 1994;91:1632–1636.
45. Xiang M, Zhou L, Macke JP, et al. The Brn-3 family of POU-domain factors: primary structure, binding specificity, and expression in subsets of retinal ganglion cells and somatosensory neurons. *J Neurosci.* 1995;15:4762–4785.
46. Drager UC, Hofbauer A. Antibodies to heavy neurofilament subunit detect a subpopulation of damaged ganglion cells in retina. *Nature.* 1984;309:624–626.
47. Levkovitch-Verbin H, Quigley HA, Martin KR, Zack DJ, Pease ME, Valenta DF. A model to study differences between primary and secondary degeneration of retinal ganglion cells in rats by partial optic nerve transection. *Invest Ophthalmol Vis Sci.* 2003;44:3388–3393.
48. Fileta JB, Huang W, Kwon GP, et al. Efficient estimation of retinal ganglion cell number: a stereological approach. *J Neurosci Methods.* 2008;170:1–8.
49. Ko ML, Hu DN, Ritch R, Sharma SC, Chen CF. Patterns of retinal ganglion cell survival after brain-derived neurotrophic factor administration in hypertensive eyes of rats. *Neurosci Lett.* 2001;305:139–142.
50. Siu AW, Leung MC, To CH, Siu FK, Ji JZ, So KF. Total retinal nitric oxide production is increased in intraocular pressure-elevated rats. *Exp Eye Res.* 2002;75:401–406.
51. Budram-Mahadeo V, Morris PJ, Latchman DS. The Brn-3a transcription factor inhibits the pro-apoptotic effect of p53 and enhances cell cycle arrest by differentially regulating the activity of the p53 target genes encoding Bax and p21(CIP1/Waf1). *Oncogene.* 2002;21:6123–6131.
52. Hudson CD, Morris PJ, Latchman DS, Budhram-Mahadeo VS. Brn-3a transcription factor blocks p53-mediated activation of proapoptotic target genes Noxa and Bax in vitro and in vivo to determine cell fate. *J Biol Chem.* 2005;280:11851–11858.
53. Latchman DS. The Brn-3a transcription factor. *Int J Biochem Cell Biol.* 1998;30:1153–1157.
54. Farooqui-Kabir SR, Budhram-Mahadeo V, Lewis H, Latchman DS, Marber MS, Heads RJ. Regulation of Hsp27 expression and cell survival by the POU transcription factor Brn3a. *Cell Death Differ.* 2004;11:1242–1244.